

The latest release of the lava flows simulation model SCIARA: first application to Mt Etna (Italy) and solution of the anisotropic flow direction problem on an ideal surface

William Spataro^{a,c}, Maria V. Avolio^a, Valeria Lupiano^b, Giuseppe A. Trunfio^d,
Rocco Rongo^{b,c}, Donato D'Ambrosio^{a,c*}

^aDepartment of Mathematics, University of Calabria, Rende, Italy

^bDepartment of Earth Sciences, University of Calabria, Rende, Italy

^cHigh Performance Computing Centre, University of Calabria, Rende, Italy

^dDepartment of Architecture and Planning, University of Sassari, Alghero, Italy

Abstract

This paper presents the latest developments of the deterministic Macroscopic Cellular Automata model SCIARA for simulating lava flows. A Bingham-like rheology has been introduced for the first time as part of the Minimization Algorithm of the Differences, which is applied for computing lava outflows from the generic cell towards its neighbours. The hexagonal cellular space adopted in the previous releases of the model for mitigating the anisotropic flow direction problem has been replaced by a - Moore neighbourhood - square one, nevertheless by producing an even better solution for the anisotropic effect. Furthermore, many improvements have been introduced concerning the important modelling aspect of lava cooling. The model has been tested with encouraging results by considering both a real case of study, the 2006 lava flows at Mt Etna (Italy), and an ideal surface, namely a 5° inclined plane, in order to evaluate the magnitude of the anisotropic effect. As a matter of fact, notwithstanding a preliminary calibration, the model demonstrated to be more accurate than its predecessors, providing the best results ever obtained on the simulation of the considered real case of study. Eventually, experiments performed on the inclined plane have pointed out how this release of SCIARA does not present the typical anisotropic problem of deterministic Cellular Automata models for fluids on ideal surfaces.

© 2010 Published by Elsevier Ltd.

Keywords: Macroscopic Cellular Automata, Numerical Simulation, Modelling, Lava Flows, Mt Etna, Anisotropy Problem.

1. Introduction

Cellular Automata (CA) [1] are parallel computing models powerful as Turing machines [2,3,4], widely utilized for modelling and simulating complex systems, whose evolution can be described in terms of local interactions.

* Corresponding author. Tel.: +39-0984-493691; fax: +39-0984-493570.

E-mail address: d.dambrosio@unical.it.

Besides theoretical studies [5], CA have been applied to a variety of fields such as pattern recognition [6,7], image processing [8] and cryptography [9]. However, major interest for CA regard their use in Complex Systems modelling in various fields like Physics, Biology, Earth Sciences and Engineering (see e.g. [10,11,12,13,14,15,16]). For instance, physicists and biologists are applying CA in their domains due to the fact that, although having a simple structure, they show a rich dynamical behaviour, which is typical of real systems. Among diverse practical usages, Fluid-dynamics is an important field of application for CA. In Physics, Lattice Gas Automata models [17] were introduced for describing the motion and collision of “particles” on a grid. It was shown that such models can simulate fluid dynamical properties. The continuum limit of these models leads to the Navier-Stokes equations. Lattice Gas models can be regarded as “microscopic” models, as they describe the motion of fluid “particles” - actually “fluid tokens” - which interact by scattering. An advantage of Lattice Gas models is that the simplicity of particles, and of their interactions, allow for the simulation of a large number of them, making it therefore possible to observe the emergence of flow patterns. A different approach characterises the so-called Lattice Boltzmann models [18,19] in which the state variables can take continuous values, as they are supposed to represent the density of fluid particles, endowed with certain properties, located in each cell (here space and time are discrete, as in lattice gas models). Both Lattice Gas and Lattice Boltzmann Models have been applied for the description of fluid turbulence (cf. [11,16]).

On the other hand, many complex natural phenomena evolve on very large areas and are therefore difficult to be modelled at a microscopic level of description. Among these, lava flows can be considered, at the same time, one of the most dangerous and difficult phenomena to be modelled as, for instance, temperature drops along the path by locally modifying the magma dynamical behaviour (because of the effect of the strong temperature-dependence of viscosity – see e.g. [20]). Lava flows generally evolve on complex topographies that can change during eruptions, due to lava solidification, and are often characterized by branching and rejoining of the flow. Furthermore, they are generally characterized by non-Newtonian rheology and there is a not complete agreement about their governing dynamics and parameters among Researchers.

Nevertheless, many attempts of modelling real cases can be found in literature. Crisci and co-workers were the first to adopt CA for modelling Etnean lava flows (Italy) through the numerical simulation code SCIARA, initially fully three-dimensional [21] and subsequently reduced to a two-dimensional CA [22], while Ishihara et al. [23] were the first to adopt a Binghamian rheology in a CA numerical code, with good results on the simulation of some lava flows in Japan. Subsequently, Miyamoto and Sasaki [24] proposed a non-deterministic CA model that, thanks to a Monte Carlo approach, did not present the anisotropic problem due to the discretization of the considered (square) cellular space. Afterwards, a similar - non deterministic - approach was adopted by Vicari et al. [25] by the CA model MAGFLOW with good results on the simulation of Etnean lava flows (cf. also [26,27]).

In this paper, we present the latest release of the CA model SCIARA, which differs with respect to its predecessor as it re-introduces square cells and adopts a Bingham-like rheology. The model showed to be able to reproduce Etnean lava flows with high accuracy, also keeping the great computational efficiency that characterised the previous releases (cf.[28]). Furthermore, although the model is fully deterministic, it showed a substantial asymmetry-free dynamics on ideal surfaces, which we attribute to both the effect of the considered rheological model and to some improvements in the considered flow distribution algorithms.

In the next section Macroscopic Cellular Automata are briefly described, while the new SCIARA model is illustrated in Section 3. Section 4 shows the results of the application of SCIARA to a real case occurred on Mt Etna, while Section 5 illustrates the dynamical behaviour of the model on an ideal surface. The last section concludes the paper with a general discussion and suggestions for future works.

2. Macroscopic Cellular Automata

Classical homogeneous Cellular Automata can be viewed as an n -dimensional space, subdivided in cells of uniform shape and size. Each cell embeds an identical finite automaton (fa), whose state accounts for the temporary features of the cell; Q is the finite set of states. The fa input is given by the states of a set of neighbouring cells, including the central cell itself. The neighbourhood conditions are determined by a geometrical pattern, X , which is invariant in time and space. The fa have an identical state transition function $\tau: Q^{\#X} \rightarrow Q$, which is simultaneously applied to each cell. At step $t=0$, fa are in arbitrary states and the CA evolves by changing the state of all fa simultaneously at discrete times, according to τ . Formally, a homogeneous CA is a 4-tuple:

$$A = \langle R, X, Q, \tau \rangle$$

Regarding the modelling of some natural complex phenomena, Crisci and co-workers proposed an extended notion of homogeneous CA, firstly applied to the simulation of basaltic lava flows [21], which makes the modelling of spatially extended systems more straightforward and overcomes some unstated limits of the classical CA such as having few states and look-up table transition functions (cf. [29]). Mainly for this reason, the method is known as Macroscopic Cellular Automata (MCA). MCA were in fact adopted for the simulation of many macroscopic phenomena, such as lava flows [28], debris flows [13], density currents [30,31], water flux in unsaturated soils [32], soil erosion/degradation by rainfall [33,34] as well as pyroclastic flows [35], bioremediation processes [14,36] and forest fires [37]. Nevertheless, despite the name, MCA have also been employed for the modelling of systems at micro/meso-scopic levels of description [38,39]. Formally, a MCA is a 7-tuple:

$$A = \langle R, X, Q, P, \tau, G, \gamma \rangle$$

where, equivalently to the homogeneous CA definition, R , Q , X and τ are the n -dimensional cellular space, the set of states of the cell, the geometrical pattern that specifies the neighbourhood relationship, and the fa transition function. Nevertheless, the set Q of state of the cell is decomposed in *substates*, Q_1, Q_2, \dots, Q_r , each one representing a particular feature of the phenomenon to be modelled. The overall state of the cell is thus obtained as the Cartesian product of the considered substates:

$$Q = Q_1 \times Q_2 \times \dots \times Q_r$$

A set of *parameters*, $P = \{p_1, p_2, \dots, p_p\}$, is furthermore considered, which allow to “tune” the model for reproducing different dynamical behaviours of the phenomenon of interest. As the set of state is split in substates, also the state transition function τ is split in *elementary processes*, $\tau_1, \tau_2, \dots, \tau_s$, each one describing a particular aspect that rules the dynamic of the considered phenomenon. Eventually, $G \subset R$ is a subset of the cellular space that is subject to *external influences*, specified by the supplementary function γ . External influences were introduced in order to model features which are not easy to be described in terms of local interactions.

As stated above, many geological processes like lava or debris flows can be described in terms of local interactions and thus modelled by MCA. By opportunely discretizing the surface on which the phenomenon evolves, the dynamics of the system can be in fact described in terms of flows of some quantity from one cell to the neighbouring ones. Moreover, as the cell dimension is a constant value throughout the cellular space, it is possible to consider characteristics of the cell (i.e. substates), typically expressed in terms of volume (e.g. lava volume), in terms of thickness. This simple assumption permits to adopt a straightforward but efficacious strategy that computes outflows from the central cell to the neighbouring ones in order to minimize the non-equilibrium conditions. Historically, in the MCA approach, outflows have mainly been computed by procedures based on one of two “distribution” algorithms: the *Minimisation Algorithm of the Differences* (cf. [29]), and the *Proportional Distribution Algorithm* (cf. [40]). The first algorithm, here adopted, is briefly described in the next section.

2.1. The Minimization Algorithm of the Differences

The Minimisation Algorithm of the Differences (MAD) is based on the following assumptions:

- two parts of the considered quantity must be identified in the central cell: these are the unmovable part, $u(0)$, and the mobile part, m ;
- only m can be distributed to the adjacent cells. Let $f(x, y)$ denote the flow from cell x to cell y ; m can be written as:

$$m = \sum_{i=0}^{\#X} f(0, i)$$

where $f(0, 0)$ is the part which is not distributed, and $\#X$ is the number of cells belonging to the X neighbourhood;

- the quantities in the adjacent cells, $u(i)$ ($i = 1, 2, \dots, \#X$) are considered unmovable;
- let $c(i) = u(i) + f(0, i)$ ($i = 0, 1, \dots, \#X$) be the new quantity content in the i -th neighbouring cell after the distribution; let c_{\min} be the minimum value of $c(i)$ ($i = 0, 1, \dots, \#X$). The outflows are computed in order to minimise the following expression:

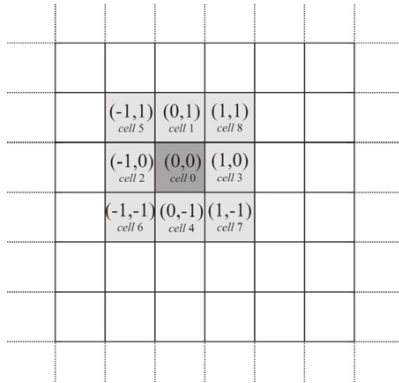


Fig. 1. Example of SCIARA cellular space and neighbourhood. Cell's integer coordinates (in brackets) and indices are shown.

$$\sum_{i=0}^{\#X} (c(i) - c_{\min}) \quad (1)$$

The MAD operates as follows:

1. the following average is computed:

$$a = \frac{m + \sum_{i \in A} u(i)}{\#A}$$

where A is the set of not eliminated cells (i.e. those that can receive a flow); note that at the first step $\#A = \#X$;

2. cells for which $u(i) \geq a$ ($i = 0, 1, \dots, \#X$) are eliminated from the flow distribution and from the subsequent average computation;
3. the first two points are repeated until no cells are eliminated; finally, the flow from the central cell towards the i -th neighbour is computed as the difference between $u(i)$ and the last average value a :

$$f(0,i) = \begin{cases} a - u(i) & i \in A \\ 0 & i \notin A \end{cases}$$

Note that the simultaneous application of the minimization principle to each cell gives rise to the global equilibrium of the system. The correctness of the algorithm is stated in [29], i.e. it minimizes equation (1). Finally, a relaxation rate, $r_r \in [0, 1]$, can be introduced, denoting that the equilibrium conditions may not be reached in a single CA step; the obtained values of outflows are therefore multiplied by r_r (if $r_r=1$, no relaxation is induced; if $r_r=0$, there will be no outflows towards the neighbourhood).

3. The computational model

As stated in Section 1, a Bingham-like rheology has been introduced for the first time in SCIARA in spite of the previous simplified rheological model in which viscosity effects and critical height were modelled in terms of lava adherence. In this previous simplified model, depending on temperature, a fixed amount of lava cannot flow out from the cell, while the part that moves is determined by a version of the Minimization Algorithm of the Differences that does not consider the effect of viscosity (being the relaxation rate set to 1 - c.f. [28]).

Conversely, the rheology here adopted is inspired to the Bingham model and therefore the concepts of critical height and viscosity are explicitly considered. In particular, lava can flow out if and only if its thickness overcomes a critical value (critical height), so that the basal stress exceeds the yield strength. Moreover, viscosity is accounted in terms of flow relaxation rate, being this latter the parameter of the distribution algorithm that influences the amount of lava that actually leaves the cell.

Table 1. List of parameters of SCIARA with values considered for the simulation of the 2006 Etnean lava flow.

Parameter	Meaning	Unit	Best value
w	Cell side	[m]	10
t	CA clock	[s]	120
T_{sol}	Temperature of solidification	[K]	1143
T_{vent}	Temperature of extrusion	[K]	1360
r_{Tsol}	Relaxation rate at the temperature of solidification	–	0.5
r_{Tvent}	Relaxation rate at the temperature of extrusion	–	0.95
hc_{Tsol}	Critical height at the temperature of solidification	[m]	40
hc_{Tvent}	Critical height at the temperature of extrusion	[m]	1.5
δ	Cooling parameter	–	2.8
ρ	Lava density	[Kg m ⁻³]	2600
ε	Lava emissivity	–	0.9
σ	Stephan-Boltzmann constant	[J m ⁻² s ⁻¹ K ⁻⁴]	5.68·10 ⁻⁸
c_v	Specific heat	[J kg ⁻¹ K ⁻¹]	1150

In formal terms, SCIARA is defined as:

$$SCIARA = \langle R, L, X, Q, P, \tau, \gamma \rangle$$

where:

- R is the set of square cells covering the bi-dimensional finite region where the phenomenon evolves;
- $L \in R$ specifies the lava source cells (i.e. craters);
- $X = \{(0, 0), (0, 1), (-1, 0), (1, 0), (0, -1), (-1, 1), (-1, -1), (1, -1), (1, 1)\}$ identifies the pattern of cells (Moore neighbourhood) that influence the cell state change; in the following we will refer to cells by indexes 0 (for the central cell) through 8, as shown in Fig 1;
- $Q = Q_z \times Q_h \times Q_T \times Q_f^8$ is the finite set of states, considered as Cartesian product of “substates”. Their meanings are: cell altitude a.s.l., cell lava thickness, cell lava temperature, and lava thickness outflows (from the central cell toward the four adjacent cells), respectively;
- $P = \{w, t, T_{sol}, T_{vent}, r_{Tsol}, r_{Tvent}, hc_{Tsol}, hc_{Tvent}, \delta, \rho, \varepsilon, \sigma, c_v\}$ is the finite set of parameters (invariant in time and space) which affect the transition function; their meaning is illustrated in Table 1;
- $\tau: Q^7 \rightarrow Q$ is the cell deterministic transition function; it is outlined in the following sections;
- $\gamma: Q_h \times \mathbb{N} \rightarrow Q_h$ specifies the emitted lava thickness from the source cells at each step $k \in \mathbb{N}$ (\mathbb{N} is the set of natural numbers).

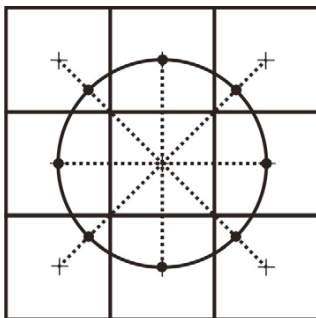


Fig. 2. Reference schema for cells altitude determination in the Moore neighbourhood. Altitudes of cells along the von Neumann neighbourhood correspond to DEM values. Those along diagonals are taken at the intersection between the diagonal line and the circle with radius w (cf. Table 1), so that the distance with respect to the centre of the central cell is constant for each adjacent neighbour.

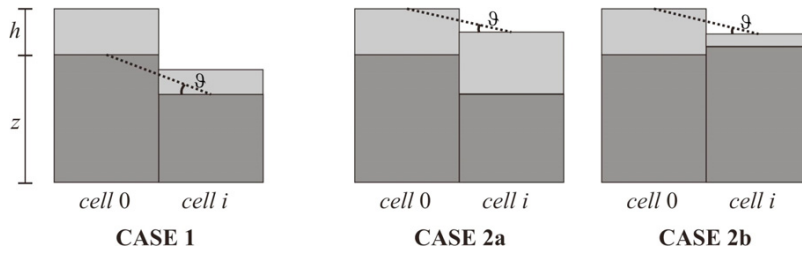


Fig. 3. Cases in which the generic neighbour (cell i) is not eliminated by the Minimisation Algorithm of the Difference and can thus receive a flow by the central cell (cell 0). Note that the slope angle θ , considered in the critical height computation, depends on the particular case.

3.1. Elementary process τ_i : lava flows computation

As stated above, viscosity is modelled in terms of flow relaxation rate, r , according to a power law of the kind:

$$\log r = a + bT \quad (2)$$

where $T \in Q_T$ is the lava temperature and the a and b coefficients determined by solving the system (cf. Table 1):

$$\begin{cases} \log r_{T_{sol}} = a + bT_{sol} \\ \log r_{T_{vent}} = a + bT_{vent} \end{cases}$$

Similarly, critical height mainly depends on lava temperature according to a power law of the kind:

$$\log h_c = c + dT \quad (3)$$

whose coefficients are obtained by solving the system (cf. Table 1):

$$\begin{cases} \log hc_{T_{sol}} = c + dT_{sol} \\ \log hc_{T_{vent}} = c + dT_{vent} \end{cases}$$

In order to apply the Minimisation Algorithm of the Differences to compute lava outflows from the central cell (which has index 0 – cf Fig. 1) to the i -th neighbour, a preliminary control is performed for “eliminating” cells that cannot receive lava due their state condition. If $\bar{z}_i \in Q_z$ is the topographic altitude and $h_i \in Q_h$ the lava thickness ($i=0, 1, \dots, \#X$), the generic cell i is not eliminated exclusively in the following two cases:

- 1) $\bar{z}_0 > \bar{z}_i \wedge h_0 \geq h_i$, i.e. both the topographic altitude of the central cell is greater than that of the neighbouring cell and the debris thickness of the central cell is greater than or equal to that of the neighbouring cell;
- 2) $(\bar{z}_0 + h_0 > \bar{z}_i + h_i) \wedge \neg(\bar{z}_0 > \bar{z}_i \wedge h_0 \geq h_i)$, i.e. the “total height” of the central cell overcomes that of the neighbouring cell, and case1) is false.

In order to solve the anisotropic problem, a fictitious topographic alteration along diagonal cells is considered with respect to those “individuated” by the DEM. In a standard situation of non-altered heights, cells along diagonals result in a lower elevation with respect to the remaining ones (which belong to the von Neumann neighbourhood), even in case of constant slope. This is due to the fact that the distance between the central cell and diagonal neighbours is greater than of the distance between the central cell and orthogonal adjacent cells (cf. Fig. 2). This introduces a side effect in the distribution algorithm, which operates on the basis of height differences. If the algorithm perceives a greater difference along diagonals, it will erroneously privilege them by producing greater outflows. In order to solve this problem, we consider the height of diagonal neighbours taken at the intersection between the diagonal line and the circle with radius w (cf. Table 1) centred in the centre of the central cell (Fig. 2). Under the commonly assumed hypothesis of inclined plane between adjacent cells (cf. [25]), this solution permits to have constant differences in level in correspondence of constant slopes, and the distribution algorithm can work properly even on the Moore neighbourhood. According to this strategy, the topographic altitude in the previous case 1) and case 2) conditions is (cf. also Fig. 1):

$$\bar{z}_i = \begin{cases} z_i & i = 0, 1, \dots, 4 \\ z_0 - (z_0 - z_i)/\sqrt{2} & i = 5, 6, \dots, \#X \end{cases} \quad (4)$$

Case 1) indicates the situation in which lava moves downslope and a lower amount of lava is found in the neighbouring cell. In this case, lava in the neighbour does not represent an obstacle. Consequently, the distribution algorithm considers only the topographic elevation of the neighbour as unmovable part $u(i)$ (cf. Section 2.1) and the slope angle, ϑ , is computed accordingly (cf. Fig. 3 - CASE 1).

Case 2) indicates the situation in which lava moves down or up-slope and lava in the neighbouring cell represents an obstacle. In fact, if $\bar{z}_0 > \bar{z}_i$ (lava moves downslope), $h_i > h_0$ must hold, which can indicate a situation where lava motion is slowing down, for instance due to cooling or because a counter-slope begins (cf. Fig. 3 - CASE 2a). Still, if $\bar{z}_0 < \bar{z}_i$, lava moves upslope and both neighbouring altitude and lava content oppose to lava motion (cf. Fig. 3 - CASE 2b). In these cases, the distribution algorithm considers both the topographic elevation and lava content of the neighbours as $u(i)$ (cf. Section 2.1) and the slope angle, ϑ , is computed accordingly (cf. Fig. 3 - CASE 2a and CASE 2b).

As a result, in order to compute lava outflows from the central cell towards its neighbours, the Minimisation Algorithm of the Differences is applied to the following quantities:

$$u(0) = \bar{z}_0;$$

$$m = h_0;$$

$$u(i) = \begin{cases} \bar{z}_i & \text{for case 1} \\ \bar{z}_i + h_i & \text{for case 2} \end{cases} \quad i = 1, 2, \dots, \#X;$$

The application of the algorithm determines the computation of flows $f(0,i)$ from the central cell to the i -th neighbour. According to the Bingham-like rheology here adopted, actual lava outflows, $h(0,i)$, are computed as:

$$h(0,i) = \begin{cases} f(0,i) \cdot r & h_0 > hc \cdot \cos \vartheta \\ 0 & h_0 \leq hc \cdot \cos \vartheta \end{cases}$$

being ϑ the slope angle, as shown in Fig. 3. The relaxation rate factor, r , computed according to equation (2), here plays the role of the viscosity in the context of the Minimization Algorithm, while the critical height, hc , computed according to equation (3), has the same meaning as that of a Bingham fluid.

3.2. Elementary process τ_2 : temperature variation and lava solidification

A two step process determines the new cell lava temperature. In the first one, the temperature is obtained as weighted average of residual lava inside the cell and lava inflows from neighbouring ones:

$$T_{avg} = \frac{h_r T_0 + \sum_{i=1}^6 h(i,0) T_i}{h_r + \sum_{i=1}^6 h(i,0)}$$

where $h_r \in Q_h$ is the residual lava thickness inside the central cell after the outflows distribution, $T \in Q_T$ is the lava temperature and $h(i,0)$ the lava inflow from the i -th neighbouring cell. Note that $h(i,0)$ is equal to the lava outflow from the i -th neighbouring cell towards the central one, computed by means of the Minimisation Algorithm. A further step updates the calculated temperature by considering thermal energy loss due to lava surface radiation [41]:

$$T = \frac{T_{avg}}{\sqrt[3]{1 + \frac{3T_{avg}^3 \epsilon \sigma t \delta}{\rho c_v w^2}}}$$

where ϵ , σ , t , δ , ρ , c_v and w are the lava emissivity, the Stephan-Boltzmann constant, the CA clock, the cooling parameter, the lava density, the specific heat and the cell side, respectively (cf. Table 1).

When the lava temperature drops below the threshold T_{sol} , lava solidifies. Consequently, the cell altitude increases by an amount equal to lava thickness and new lava thickness is set to zero.

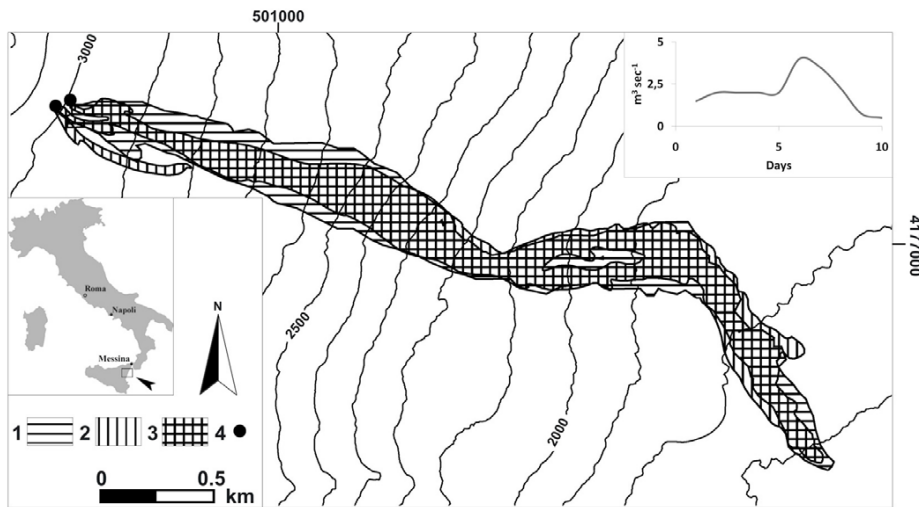


Fig. 4. Simulation of the 2006 Etnean lava flow by the CA model SCIARA. Key: 1) simulated event; 2) real event; 3) overlapping area between real and simulated events; 4) lava vents sources. The effusion rate is shown in the upper right corner of the figure.

4. First simulations at Mt Etna: the 2006 Valle del Bove Lava Flow

Etna's July 2006 eruption began during the night of 14 July, when a fissure opened on the east flank of the South-East Crater. Two vents (cf. key 4 of Fig. 4) fed lava flow towards east into the Valle del Bove. The effusion rate trend here adopted is in agreement with that considered by Neri et al. [42] and is shown in Fig. 4.

A preliminary calibration allowed to individuate values for model's parameters, which are listed in Table 1. The corresponding CA simulation, performed on a 10m cell size DEM of 797 columns and 517 rows, is shown in Fig. 4. In order to quantitatively evaluate the goodness of our simulation, we adopted the e_1 fitness function, which provides a measure of the overlapping (in terms of areal extent) between the real and simulated event. Let us denote with R and S the sets of CA cells affected by the real and simulated event, respectively. Let $m(R \cap S)$ and $m(R \cup S)$ be the measure of their intersection and union, respectively. The fitness function e_1 is defined as follows:

$$e_1 = \sqrt{\frac{m(R \cap S)}{m(R \cup S)}}$$

Note that the function e_1 gives values belonging to the interval $[0, 1]$. Its value is 0 if the actual and simulated events are completely disjoint, being $m(R \cap S) = 0$; it is 1 in case of a perfect overlap, being $m(R \cap S) = m(R \cup S)$.

As the Fig. 4 shows, the simulation does not differ significantly from the real case, as confirmed by the more than satisfying value of the fitness function, $e_1 = 0.8$. The goodness of the simulation is also confirmed in terms of run-out, as the travelled distance from the sources of the simulated event is practically the same as the real one.

5. Simulations on ideal surfaces

In general, deterministic CA for the simulation of macroscopic fluids present a strong dependence on the cell geometry and directions of the cellular space. We have already evidenced that, due to the discretization of the surface where the phenomenon evolves, diagonal cells can be greatly privileged in flow distribution and thus lava can spread preferentially in these directions.

In order to solve the problem, different solutions have been proposed in literature, such as the adoption of hexagonal cells (e.g. [12,43,44]) or Monte Carlo approaches (e.g. [24,25]). The first solution, however, does not solve perfectly the problem on ideal surfaces, while the second one has the disadvantage of giving rise to non-deterministic simulation models.

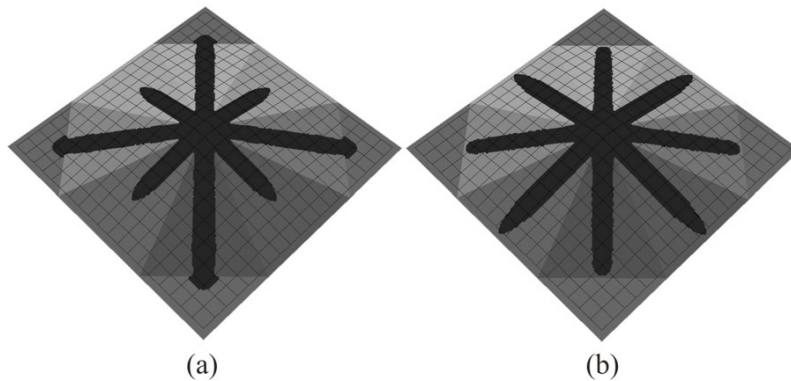


Fig. 5. SCIARA simulations on an octagonal-base pyramid with faces inclined by an angle $\alpha = 5^\circ$, performed for evaluating the anisotropic flow direction problem: a) case in which actual cell topographic elevations are considered; b) case in which equation (4) is applied and topographic corrections along diagonals considered. Note that the square lattice in both figures is only indicative of the cellular space orientation and does not correspond to the actual cellular space in terms of number of rows and columns.

Here we show that the present deterministic release of SCIARA does not present the anisotropic problem on an ideal surface, represented by an octagonal-base pyramid having faces inclined by an angle $\alpha = 5^\circ$. The pyramid is represented by a 10m cell size DEM of 203 columns and 203 rows. By locating the lava source at the top of the structure, both flows along diagonals and orthogonal directions of the square cellular space are observed. Figure 5 shows the results of two test cases in which a constant effusion rate, equal to $1 \text{ m}^3 \text{ s}^{-1}$, is emitted for a total of 6 days, and no temperature loss is considered. The first simulation is obtained by considering the actual topographic heights of the cells, while the second by taking into account the topographic corrections discussed in section 3.1 - cf. equation (4). As it can be seen, the anisotropic problem is quite significant in the first case, in which diagonal flows, as expected, reach the base of the pyramid more rapidly with respect to those on the orthogonal directions. In the second case, in which topographic alteration are considered, the problem is practically absent and all flows reach the base of the pyramid at the same moment.

6. Discussion

We have presented the latest release of the Macroscopic Cellular Automata model SCIARA for simulating lava flows. For the first time in the SCIARA family of lava flows models, this release considers a Bingham-like rheology. Moreover, it re-introduces a square tessellation of the cellular space instead of the previously adopted hexagonal one, which was considered in the earlier versions to limit the effect of the anisotropic flow direction problem. Notwithstanding, we have shown that the model is able to solve the problem on an ideal inclined surface. This result is particularly significant, being SCIARA a deterministic model, as all the previously proposed solutions refer to probabilistic CA simulation models.

A preliminary calibration also allowed to reproduce a real case of study, namely the 2006 lava flows at Mt Etna (Italy), with a great level of accuracy. In fact, a high degree of overlapping between the real and the simulated event and a perfect fitting in terms of run-out were obtained.

Anyhow, these encouraging preliminary results need to be confirmed by further analysis. First of all, a more thorough calibration phase is required, together with a related validation one, in order to assess the validity and reliability of the model in simulating real cases of study. A further sensitivity analysis must also be performed for evaluating, in particular, the numerical stability of the model. Eventually, further tests on different ideal surfaces, e.g. planes with different inclinations, should be performed in order to better evaluate the behaviour of the model with respect flow anisotropy.

References

1. J. von Neumann, Theory of self reproducing automata, University of Illinois Press, Urbana, 1966.
2. E.F. Codd, Cellular Automata. Academic Press, New York, 1968.
3. E. Berlekamp, J.H. Conway, R. Guy, Winning for Your Mathematical Plays, Academic Press, New York, 1982.
4. E. Fredkin, T. Toffoli, Intern. J. Theor. Phys. 21 (1982) 219–253.
5. S. Wolfram, A new kind of Science, Wolfram Media Inc., Champaign, USA, 2002.
6. D. Merkle and T. Worsch, Fund. Inform. 52 (2002) 183–201.
7. P. Maji, C. Shaw, N. Ganguly, B.K. Sikdar, P.P. Chaudhuri, Fund. Inform. 58 (2003) 321–354.
8. P.L. Rosin, IEEE Trans. In. Proc. 15 (2006) 2076–2087.
9. M. Tomassini and M. Perrenoud, Appl. Soft Comp. 1 (2001) 151–160.
10. M. Avolio, G.M. Crisci, S. Di Gregorio, R. Rongo, W. Spataro, D. D'Ambrosio, Comp. Geosc. 32 (2006) 897–911.
11. B. Chopard and M. Droz, Cellular Automata Modeling of Physical Systems. Cambridge University Press, 1998.
12. G.M. Crisci, R. Rongo, S. Di Gregorio, W. Spataro, J. Volcan. Geoth. Res. 132 (2004) 253–267.
13. D. D'Ambrosio, W. Spataro, G. Iovine, H. Miyamoto, Environ. Model. Soft. 22 (2007) 1417–1436.
14. S. Di Gregorio, R. Serra, M. Villani, Comp. Sys. 11 (1997) 31–54.
15. J.R. Weimar, Fund. Inform. 52 (1966) 277–284.
16. S. Succi, The Lattice Boltzmann Equation for Fluid Dynamics and Beyond, Oxford University Press, 2004.
17. J. Hardy, Y. Pomeau, G. de Pazzis, J. Math. Phys. A, 13 (1976) 1949–1961.
18. G. McNamara, G. Zanetti, Phys. Rev. Lett., 61 (1988) 2332–2335.
19. F. Higuera, J. Jimenez, Europhys. Lett. 9 (1989) 663–668.
20. E. Costa, G. Macedonio, Nonlin. Proc. Geophy. 10 (2003) 545–555.
21. G.M. Crisci, S. Di Gregorio, G. Ranieri, in Proc. Inter. AMSE Conf. Model. Simul. Paris, France, Jul.1-3, 1982.
22. D. Barca, G.M. Crisci, S. Di Gregorio, S. Marabini, F.P. Nicoletta, Proceedings of the Kagoshima International Conference on Volcanoes, (1988) 475–478.
23. K. Ishihara, M. Iguchi, K. Kamo, in: J.K. Fink (eds.) Lava flows and domes: emplacement mechanisms and hazard implications. Springer, Berlin Heidelberg: New York, 1990.
24. H. Miyamoto and S. Sasaki, Comp. Geosc. 23 (1997) 283–292.
25. A. Vicari, A. Herault, C. Del Negro, M. Coltelli, M. Marsella, C. Proietti, Environ. Model. Soft. 22 (2007) 1465–1471.
26. C. Del Negro, L. Fortuna, A. Herault, A. Vicari, Bull. Volcan. 70 (2008) 805–812.
27. A. Vicari, A. Ciraudo, C. Del Negro, A. Herault, L. Fontana, Nat. Haz. 50 (2008) 539–550.
28. R. Rongo, W. Spataro, D. D'Ambrosio, M.V. Avolio, G.A. Trunfio, S. Di Gregorio, Fund. Inform. 87 (2008) 247–268.
29. S. Di Gregorio and R. Serra, Fut. Gener. Comp. Sys., 16 (1999) 259–271.
30. T. Salles, S. Lopez, M.C. Caca, T. Mulder, Geomorph. 88 (2007) 1–20.
31. T. Salles, T. Mulde, M. Gaudin, M.C. Cacas, S. Lopez, P. Cirac, Geomorph. 97 (2008) 516–537.
32. G. Folino, G. Mendicino, A. Senatore, G. Spezzano, S. Straface, Paral. Comp. 32 (2006) 357–376.
33. D. D'Ambrosio, S. di Gregorio, Gabriele S. Gaudio R., Phy. Chem. Ear., Part B, 26 (2001) 33–40.
34. G. Valette, S. Prévost, L. Lucas, J. Léonard, Comp. Graph. 30 (2006) 494–506.
35. M.V. Avolio, G.M. Crisci, S. Di Gregorio, R. Rongo, W. Spataro, D. D'Ambrosio, Comp. Geosc. 32 (2006) 897–911.
36. M. Andretta, R. Serra, M. Villani, Comp. Geosc. 32 (2006) 890–896.
37. G. A. Trunfio, Lect. Not. Comp. Sc. 3305 (2004) 385–394.
38. S. Di Gregorio, R. Rongo, W. Spataro, W., G. Spezzano, D. Talia, Comp. Scien. Engin. 3 (1996) 33–43.
39. S. Di Gregorio, R. Umeton, A. Bicocchi, A. Evangelisti, M.A. Gonzales, Proc. Inter. Work. Model. Appl. Simul., Campora San Giovanni, Amantea (CS), Italy, (2008) 665–674.
40. S. Di Gregorio, R. Rongo C. Siciliano M. Sorriso-Valvo, W. Spataro, Phy. Chem. Ear., Part A, 24 (1999) 97–100.
41. S. Park and J.D. Iversen, Geophys. Res. Lett. 11 (1984).
42. M. Neri, B. Behncke, M. Burton, G. Galli, S. Giammanco, E. Pecora et al., Geophys. Res. Lett. 33 (2006).
43. M. Avolio, S. Di Gregorio, R. Rongo, M. Sorriso-Valvo, W. Spataro, in A. Buccianti, G. Nardi, R. Potenza (eds), Litografia Editrice, Naples, 1998.
44. D. D'Ambrosio, S. Di Gregorio, G. Iovine, Nat. Haz. Ear. Sys. Sc. 3 (2003) 545–559.